Journal of Biomedical Optics

SPIEDigitalLibrary.org/jbo

Stepwise multiphoton activation fluorescence reveals a new method of melanin detection

Zhenhua Lai
Josef Kerimo
Yair Mega
Charles A. DiMarzio

SPIE

Stepwise multiphoton activation fluorescence reveals a new method of melanin detection

Zhenhua Lai,[a,c] Josef Kerimo,[a,c] Yair Mega,[a,c] and Charles A. DiMarzio[a,b,c]
[a]Northeastern University, Electrical and Computer Engineering Department, Boston, Massachusetts 02115
[b]Northeastern University, Mechanical Engineering Department, Boston, Massachusetts 02115
[c]Northeastern University, Bernard M. Gordon Center for Subsurface Sensing and Imaging System, Boston, Massachusetts 02115

Abstract. The stepwise multiphoton activated fluorescence (SMPAF) of melanin, activated by a continuous-wave mode near infrared (NIR) laser, reveals a broad spectrum extending from the visible spectra to the NIR and has potential application for a low-cost, reliable method of detecting melanin. SMPAF images of melanin in mouse hair and skin are compared with conventional multiphoton fluorescence microscopy and confocal reflectance microscopy (CRM). By combining CRM with SMPAF, we can locate melanin reliably. However, we have the added benefit of eliminating background interference from other components inside mouse hair and skin. The melanin SMPAF signal from the mouse hair is a mixture of a two-photon process and a third-order process. The melanin SMPAF emission spectrum is activated by a 1505.9-nm laser light, and the resulting spectrum has a peak at 960 nm. The discovery of the emission peak may lead to a more energy-efficient method of background-free melanin detection with less photo-bleaching. [DOI: 10.1117/1.JBO.18.6.061225]

Keywords: fluorescence; stepwise multiphoton excitation; melanin; microscopy; near-infrared.

Paper 12599SS received Sep. 10, 2012; revised manuscript received Dec. 1, 2012; accepted for publication Dec. 5, 2012; published online Jan. 7, 2013.

1 Introduction

Melanin is the characteristic chromophore of human skin with various biological functions, which include protection from solar radiation,[1–3] antioxidant defense, and camouflage.[4] Melanin is also involved in skin diseases such as malignant melanoma, an aggressive skin cancer with high metastatic potential. Despite its importance, melanin is poorly understood, because it is an insoluble polymer without a well-defined structure, making it difficult to isolate and study.[5] Naturally occurring pigmentation that determines hair, eye, and skin coloration is attributed to two types of melanin: eumelanin and pheomelanin. Eumelanin is the dominant component of brown and black pigments in dark skin and black hair, while pheomelanin is more common in yellow and red pigments in hair.[6] Eumelanin is the most prevalent and important form of melanin and has been the most intensively studied.[7,8] X-ray scattering and tunneling microscopy experiments have suggested that oligomers of four to six indole species form and may represent a fundamental structural unit of eumelanin termed a "protomolecule."[9,10] Theoretical models of eumelanin protomolecules and their optical properties have also been studied.[11] Atomic force and scanning electron microscopy have shown that the organization of melanin into various sizes, from tens of nanometers to micrometers, plays an important role in its function and photophysics.[12]

Various microscopy methods have been used to study melanin. For confocal scanning laser microscopy of live human skin, melanin provides strong contrast.[13] Optical spectroscopy is a commonly used method of studying the optical properties of melanin.[14,15] Near-infrared (NIR) autofluorescence imaging shows that cutaneous melanin in pigmented skin disorders emits higher NIR autofluorescence than surrounding normal tissue.[16]

In general, melanin is considered a weak emitter with a very low quantum yield of fluorescence:[17] less than 10^{-3}. Previous research has shown that stepwise two-photon excitation of melanin fluorescence can be generated by an 800-nm, 120-fs-pulse laser with an emission spectrum that peaks at around 525 nm.[18,19] The process of stepwise two-photon excitation of melanin fluorescence is different from the generally known process of simultaneous two-photon excitation of fluorescence. The former is a two-step process via a real intermediate excitation state energy level, whereas such a real intermediate state is missing in the latter case. Stepwise two-photon excitation needs only two or more orders of magnitude lower excitation intensity to obtain the same population density of the fluorescent level as compared with simultaneous excitation.[19,20] Therefore, simultaneous two-photon excitation can only be generated using an expensive ultrafast laser, whereas stepwise two-photon excitation can be generated using a low-cost continuous wave (CW) laser such as a diode laser. Although it was claimed that the melanin fluorescence can be explained by stepwise two-photon absorption, it is still unclear whether the process is a second-order or a higher-order one. In this article, we will define this process as stepwise multiphoton excitation fluorescence (SMPEF).[21]

The melanin SMPEF observed by Teuchner and Hoffmann was weak. Therefore, it is hard to detect in hair and skin, due to the background interference from other biological components. Kerimo discovered enhanced melanin fluorescence by stepwise three-photon excitation.[20] This kind of fluorescence emits a much stronger signal than the previously reported SMPEF. In our previous work, we showed that melanin needed to be

Address all correspondence to: Zhenhua Lai, Northeastern University, Department of Electrical and Computer Engineering, 440 Dana, 360 Huntington Avenue, Boston, Massachusetts 02115. Tel: 617-373-8570; E-mail: lai.z@husky.neu.edu

0091-3286/2013/$25.00 © 2013 SPIE

activated by high photon densities in order to produce a strong SMPEF signal. Therefore, in this article, we define the process as stepwise multiphoton activated fluorescence (SMPAF) to distinguish the process discovered by Kerimo from the SMPEF observed by Teuchner and Hoffmann. Kerimo's paper was the first to examine melanin SMPEF using a CW laser.[20] Mega first used melanin SMPAF as an imaging modality in a low-cost imaging configuration.[22] The SMPAF spectra of melanin in various biological tissues and pure melanin is activated by 920-nm and 830-nm laser light in both CW and pulsed mode were measured in our previous work.[21] The melanin SMPAF spectra showed a broad distribution[21] from 450 to 700 nm and beyond, in contrast to the spectra Teuchner and Hoffmann measured. The broad spectrum extending from the visible into the NIR wavelengths reveals potential application for low-cost and reliable imaging modality for detecting melanin inside biological components. Although our imaging spectrometer had a detection wavelength range of 450 to 700 nm, the SMPAF spectra continued rising past 700 nm. It is expected that the spectrum of melanin SMPAF has a peak longer than 700 nm. The position of the spectrum peak was measured in this work with an improved spectrometer, which extends the detection range to NIR.

2 Materials and Methods

2.1 *Samples*

The eumelanin sample from Sepia for spectral measurement was purchased from the Sigma Chemical Company. The mouse hair and skin samples were from the skin of a black 6 strain laboratory mouse sacrificed in unrelated research. All mouse hair and skin samples were imaged with the Keck 3D fusion multimodal microscope. The samples were mounted inside culture dishes, so that the air could be purged with nitrogen in order to reduce photo-bleaching. To prevent dehydration of the sample, 100% relative humidity on the sample was maintained by bubbling the nitrogen through water.

2.2 *Keck 3D Fusion Multimodal Microscope*

The Keck 3D fusion multimodal microscope (3DFM) in the Optical Science Laboratory (OSL) at Northeastern University allows us to image samples with multiple modalities on the same stage.[23] The modalities on the 3DFM include differential interference contrast microscopy (DIC), confocal reflectance microscopy (CRM), confocal fluorescence microscopy (CFM), multiphoton fluorescence microscopy (MPFM), optical quadrature microscopy (OQM), and others. An imaging spectrometer is integrated in the 3DFM for spectrum measurement. In this work, only CRM and MPFM modalities are used.

The layout of the 3DFM is shown in Fig. 1. A detailed description of the microscope system can be found in Warger et al.[23] Only the modalities and functions related to this work are shown in this figure. A Tsunami Ti:Sapphire Laser from Spectra-Physics is used as the light source. A small portion (less than 10%) of light is reflected by beam splitter 1 for real-time power monitoring. The power meter (Newport, 1830C) is connected to a computer to quantify the number of photons exciting the sample. Beam splitter 2, a polarizing beam splitter, reflects light that returns from the sample and is used for the CRM. The APD (Hamamatsu, C5460) is used for detection of the CRM signal.

The XY scanner consists of a polygon scanner and a galvanometer scanner. The polygon scanner performs fast scanning along a linear direction with line speeds of roughly 6 kHz and a pixel dwell time of 200 ns, while the galvanometer scans the line in the perpendicular direction, resulting in an imaging rate of 10 frames per second.[20] Five frames were averaged on each image presented in this article for noise reduction. In the configuration of fluorescence spectra measurement and fluorescence output power dependence measurement, the galvanometer was turned off, so that the polygon scanner performs continuous line scanning at a selected location on the sample.

The quarter wave plate is used for changing the polarization of input and output light to maximize the signal to the APD through the polarizing beam splitter. The dichroic mirror reflects the fluorescence signal while passing the input and reflected laser light. The filter box contains switchable optical filters. The filters used in this work are a 460-nm filter (bandwidth 50 nm), a 525-nm filter (bandwidth 40 nm), a 620-nm filter (bandwidth 60 nm) and a broadband filter (370 to 650 nm). The selection of filters corresponds to the broad melanin SMPAF spectra previously detected.[21] The photo multiplier tube (PMT) (Hamamatsu, HC 124) is used for detection of the fluorescence signal. The linearity of the PMT was tested and corrected, as needed, by software. Brightfield images can also be taken by a camera (SPOT RT900). The imaging spectrometer consists of a 150-g/mm grating (Princeton Instruments SP2150) and the SPOT camera.

2.3 *Activation of Melanin SMPAF*

A Tsunami Ti:Sapphire Laser was used to induce the enhanced emission from the melanin and to perform the multiphoton fluorescence imaging in either pulsed or CW mode. The enhanced emission could be generated equally well in pulsed or CW mode

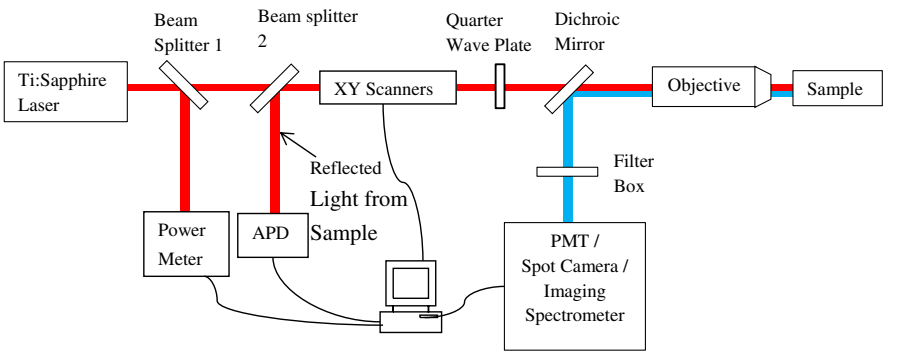

Fig. 1 Layout of the KECK 3D fusion multimodal microscope. Only modalities and functions related to this work are shown in the graph.

using the same average laser power level. The laser spot size in the system is $\sim 10^{-18}$ m^3. The procedure used by Kerimo[20] was followed to activate and image the specimen. First, a large photon density ($\geq 10^{29}$ photon/m^2) was used to activate melanin SMPAF. Once SMPAF was activated, the laser power was turned down for measurements to avoid photon-bleaching.

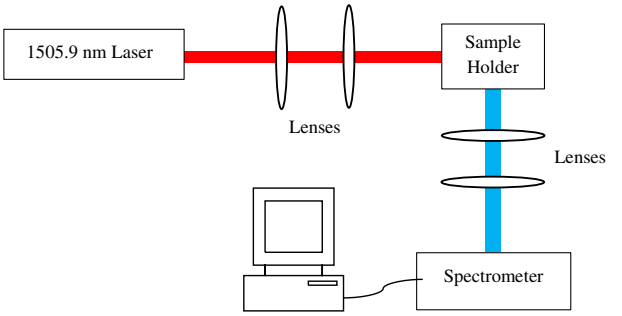

Fig. 2 Experimental setup for detection of the peak spectrum of melanin SMPAF.

2.4 *Fluorescence Spectrum Measurement*

As the spectrometer integrated in the 3DFM only works at the range of 450 to 700 nm, a separate experimental setup is utilized for detection of the peak spectrum of melanin SMPAF (Fig. 2).

A 1505.9-nm laser is used (Velocity 6300-LN) as the activation source. The monochromator (Princeton Instruments ACTON sp-2500i) consists of a 300-groove grating and a liquid-nitrogen-cooled CCD (Princeton Instruments Spec-10:400B/LN). The wavelength of the spectrometer is calibrated using the software provided by the manufacturer. The spectral intensity of the spectrometer is calibrated using a tungsten light source at a predetermined temperature (GE.Q6.6AT3).

3 Results

3.1 *SMPAF and Photo-Bleaching*

Figure 3 shows brightfield images of mouse hairs taken by the SPOT camera. The signal generated by SMPAF was strong enough that it was visible to eyesight alone. Figure 3(a) is a brightfield image of the mouse hairs before laser activation. Figure 3(b) is a brightfield image of the mouse hairs after

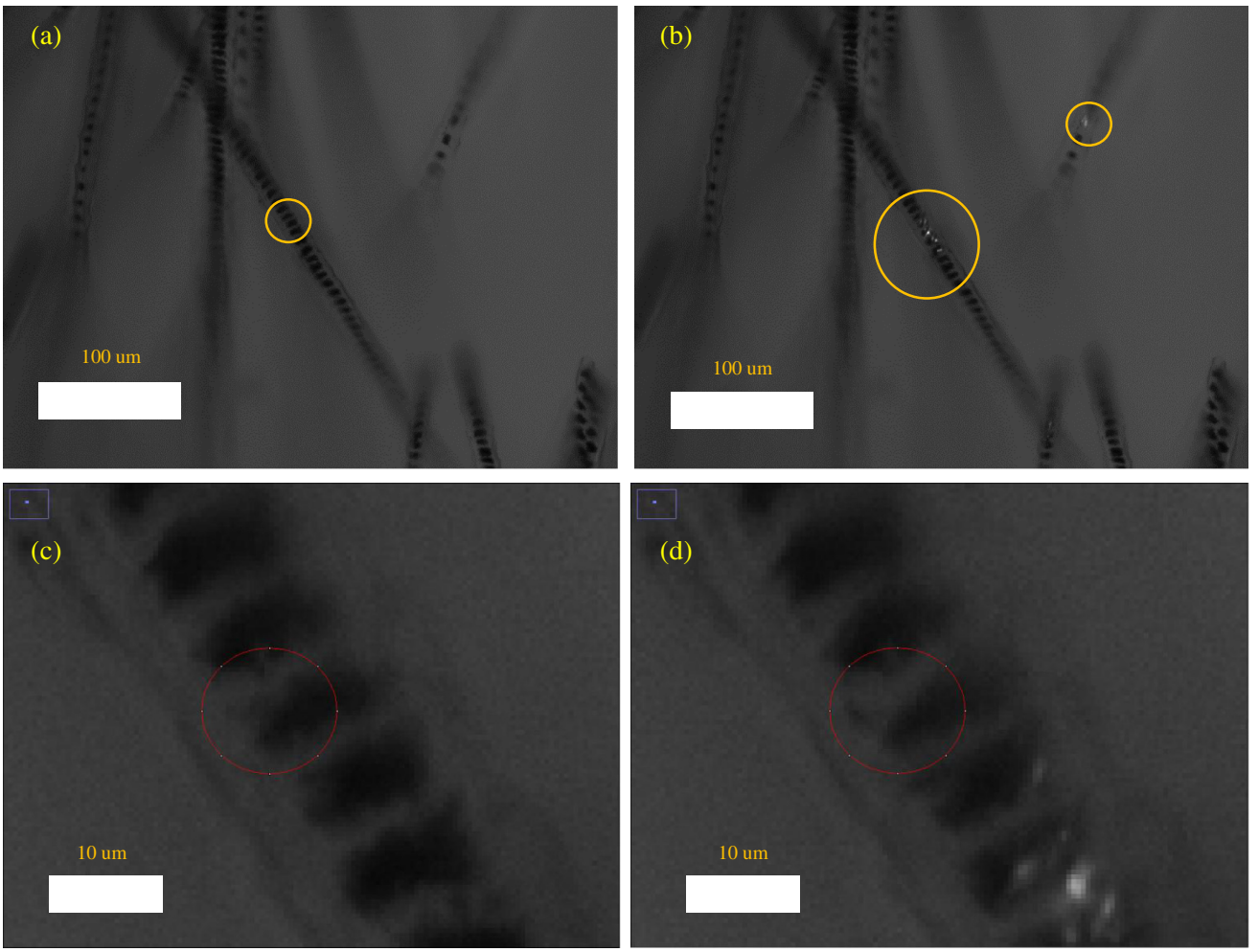

Fig. 3 Brightfield images of mouse hairs taken by the SPOT camera. The signal generated by SMPAF was strong enough that it was visible to eyesight alone. (a) Mouse hairs before laser activation. (b) Mouse hairs after laser exposure for 7 s. Within these two figures, the orange circular areas are places where melanin is activated. (c) An expanded subimage on the orange circular area in (a). (d) An expanded subimage on the orange circular area in (a) after laser exposure for 60 s. There is an obvious change to the melanin in the area of the red circle, which is consistent with our earlier report. (See Ref. 20.) The activation source used for all images was an 830-nm pulsed laser.

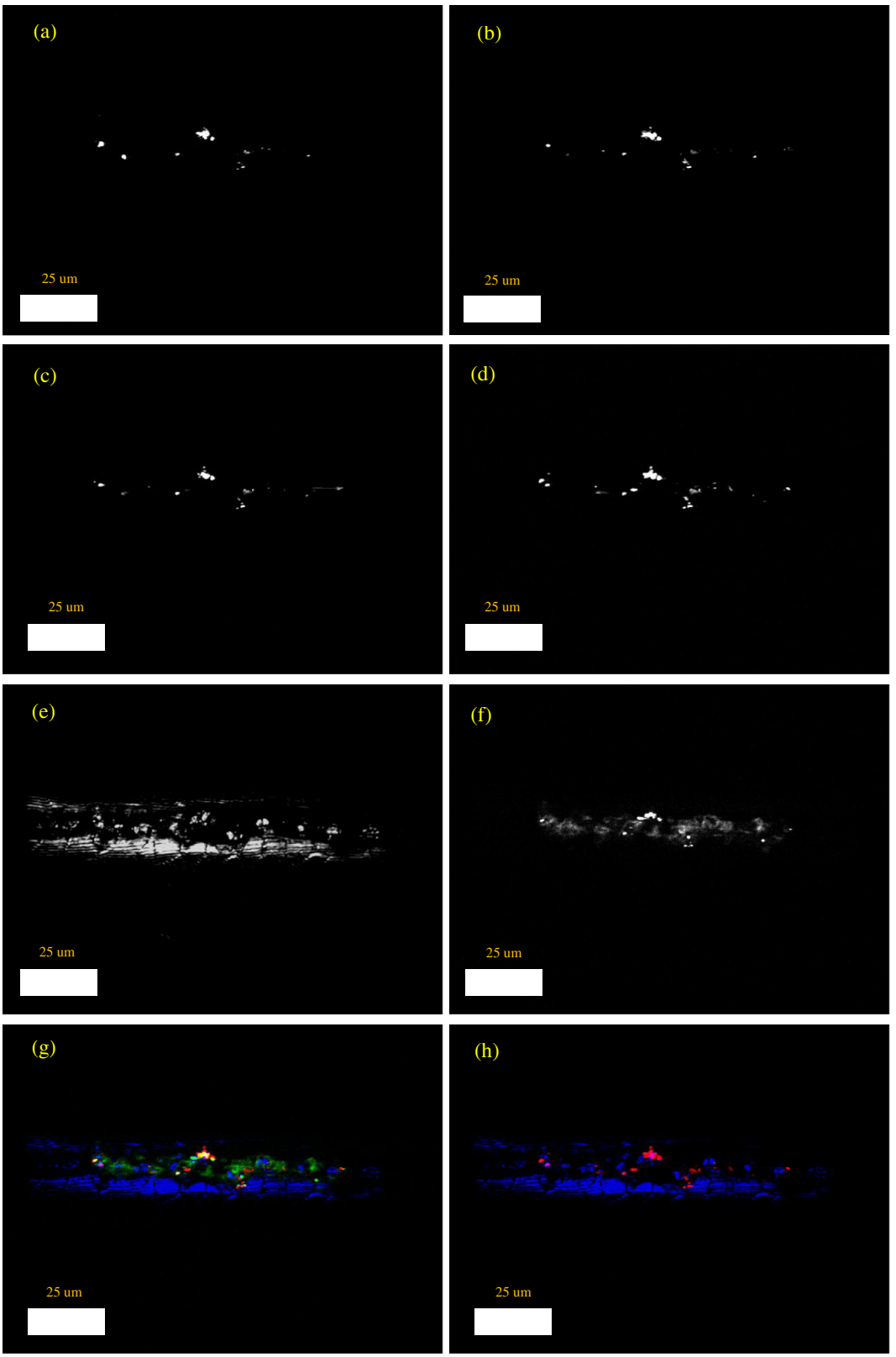

Fig. 4 Images of a mouse hair at the same position using different imaging modalities and filters. The first four images show SMPAF using a 460-nm filter (a), a 525-nm filter (b), a 620-nm filter (c) and a broadband filter (370 to 650 nm) (d). The activation source is a 920-nm CW laser. The broad distribution of the fluorescence signal activated by the CW laser matches the spectra of data we acquired previously (see Ref. 21), which confirms that the signals acquired are SMPAF images of melanin. (e) CRM image. (f) MPFM mode image using the broadband filter with activation from a 920-nm pulsed (100-fs pulse width) laser. (g) A composite image of (d) (red channel), (e) (blue channel), and (f) (green channel). The red channel shows the location of melanin SMPAF. The blue channel shows the physical structure of mouse hair, and the green channel shows the auto-fluorescence of hair components as well as SMPAF of melanin. (h) The composite image of (d) and (e). By combining CRM with SMPAF, we can locate the melanin, with respect to other hair components.

laser exposure for 7 s. Within these two figures, the orange circular areas are places where melanin is activated. Figure 3(c) is an expanded subimage on the orange circular area in Fig. 3(a). Figure 3(d) is an expanded subimage on the orange circular area in Fig. 3(a) after laser exposure for 60 s. There is an obvious change to the melanin in the area of the red circle, which is consistent with our earlier report.[20] The activation source used for all images in Fig. 3 was an 830-nm pulsed laser.

Even though the laser power is uniform at the focal plane, the time required for melanin to be activated varies. In some places, the SMPAF signal is detected immediately after laser exposure, while in other places, no SMPAF signal is detected even after laser exposure for 20 min. There is no clear understanding of how the activation time is related to any physical features of melanin. The SMPAF signal is detected by excitation of much lower laser power ($\leq 10^{28}$ photon/m^2) after laser activation. There is no SMPAF signal detected at the same power level without laser activation.

3.2 *Multimodal Microscopy*

Multimodal images of the mouse hair and skin were taken using the MPFM and CRM mode of the 3DFM. Although the laser power was turned down after activation to reduce the photo-bleaching, in order to obtain a detectable signal under different filters, a relatively high laser input power ($\sim 10^{29}$ photon/m^2) was used and maintained. Therefore, the photo-bleaching was strong.

Figure 4 shows images of a mouse hair at the same position using different imaging modalities and filters. The first four images show SMPAF using a 460-nm filter (a), a 525-nm filter (b), a 620-nm filter (c), and a broadband filter (370 to 650 nm) (d). The activation source is a 920-nm CW laser. The broad distribution of the fluorescence signal activated by the CW laser matches the spectra of data we acquired previously,[21] which confirms that the signals acquired are SMPAF images of melanin. Figure 4(e) is a CRM image. Figure 4(f) is a MPFM mode image using the broadband filter (370 to 650 nm) with activation from a 920-nm pulsed (100-fs pulse width) laser. Figure 4(g) is a composite image of Fig. 4(d) (red channel), Fig. 4(e) (blue channel), and Fig. 4(f) (green channel). The red channel shows the location of melanin SMPAF. The blue channel shows the physical structure of the mouse hair, and the green channel shows the auto-fluorescence of hair components as well as SMPAF of melanin. Figure 4(h) is the composite image of Fig. 4(d) and 4(e).

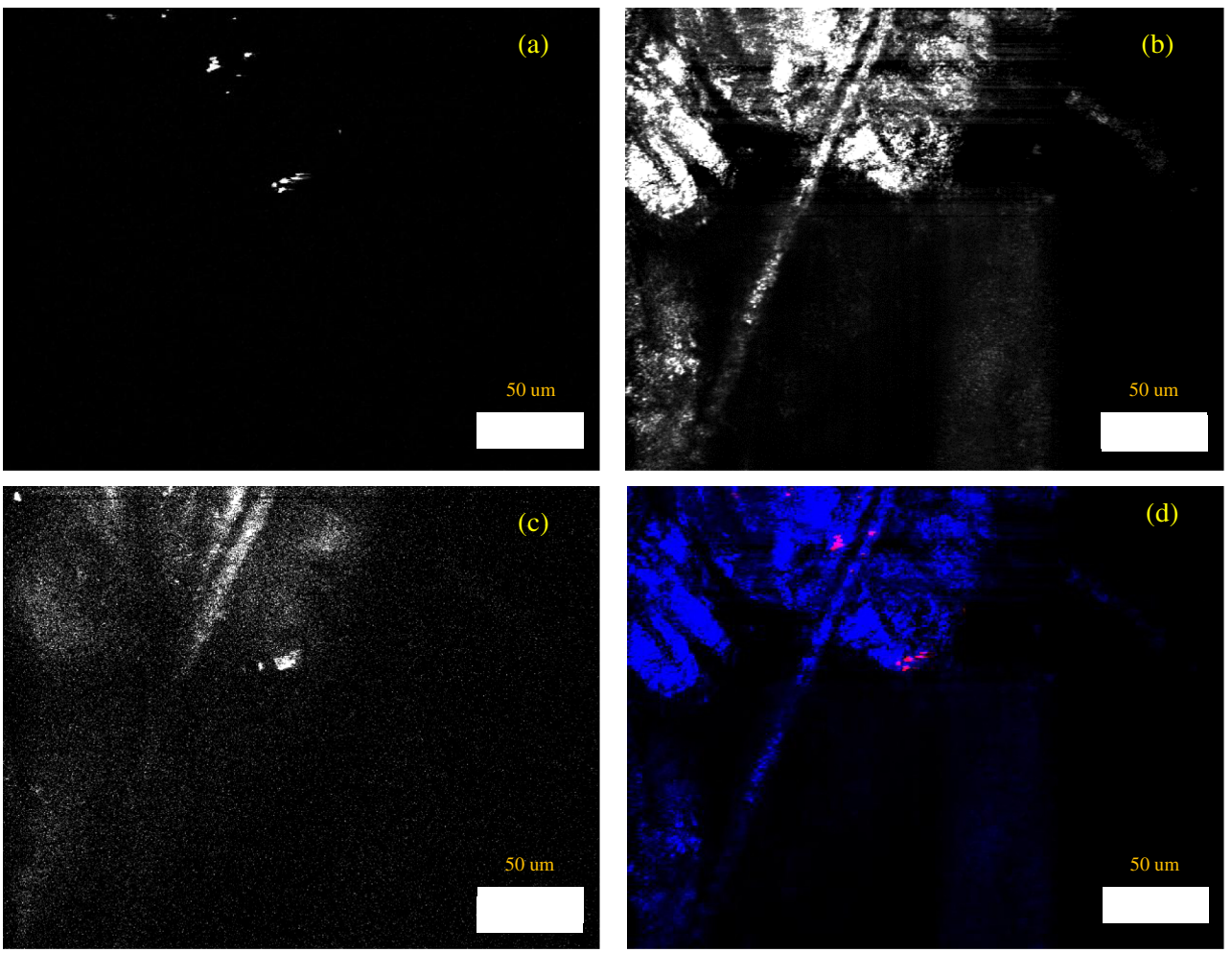

Fig. 5 Images of mouse skin at the same position using different imaging modalities. (a) An image collected using the broadband filter (370 to 650 nm) and CW laser at 920 nm. (b) The corresponding CRM image. (c) A multiphoton fluorescence image using the broadband filter activated by the 920-nm pulsed laser. It is clear the background auto-fluorescence is very high with the pulsed laser and is not present in the CW laser image. (d) A composite image of (a) (red channel) and (b) (blue channel). The red channel shows the location of melanin SMPAF, and the blue channel shows the physical structure of mouse skin.

By combining CRM with SMPAF, we can locate the melanin, with respect to other hair components.

The CW laser prevents the images in MPFM mode from being affected by the auto-fluorescence signal from other hair components. Therefore, the signal-noise-ratio (SNR) of the image is greatly increased, such that melanin is more easily detected and located. For example, the femtosecond pulsed laser generates background interference, due to the multiphoton absorption by keratin, as shown in Fig. 4(f). The CW laser image lacks this background, as can be seen in Fig. 4(a)–4(d).

The background interference was even greater when imaging mouse skin with the pulsed laser. Figure 5 shows images of mouse skin at the same position using different imaging modalities. The image in Fig. 5(a) was collected using the broadband filter (370 to 650 nm) and CW laser at 920 nm. Figure 5(b) is the corresponding CRM image. Figure 5(c) is a multiphoton fluorescence image using the broadband filter activated by the 920-nm pulsed laser. It is clear that the background auto-fluorescence is very high with the pulsed laser and is not present in the CW laser image. Figure 5(d) is a composite image of Fig. 5(a) (red channel) and Fig. 5(b) (blue channel). The red channel shows the location of melanin SMPAF, and the blue channel shows the physical structure of mouse skin.

3.3 *SMPAF Spectra and Power Dependence*

Figure 6 shows a SMPAF spectrum of mouse hair melanin. The spectrum matches the data we previously obtained on other types of melanin samples. Note that this spectrum has been corrected for the overall spectral response of the system.[21] The continuous rising slope of the spectrum indicates that the SMPAF peak of melanin must be well past 700 nm, and that even larger signal levels are to be expected when it is used to image and detect melanin. As the PMT in our microscope can detect only wavelengths less than 650 nm, a small fraction of the total SMPAF signal is detected. The peak spectrum of melanin is measured in a separate experimental setup (Fig. 2). The new setup does not allow us to image the specimen, so it is hard to locate and activate the melanin at a specific point. Instead, we used a bulk sample of pure sepia melanin as the specimen. Figure 7 shows the corrected SMPAF spectrum of sepia melanin. The sample was excited with a CW laser at 1505.9 nm, and the peak of the fluorescence spectrum is around 960 nm.

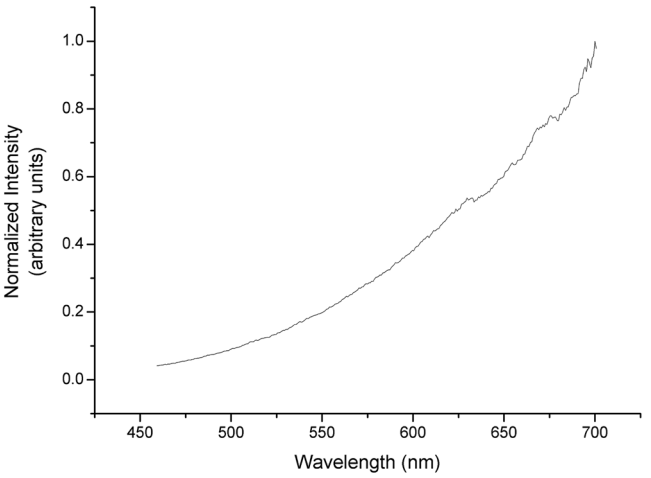

Fig. 6 SMPAF spectrum of mouse hair melanin. $\lambda_{exc} = 920$ nm, CW.

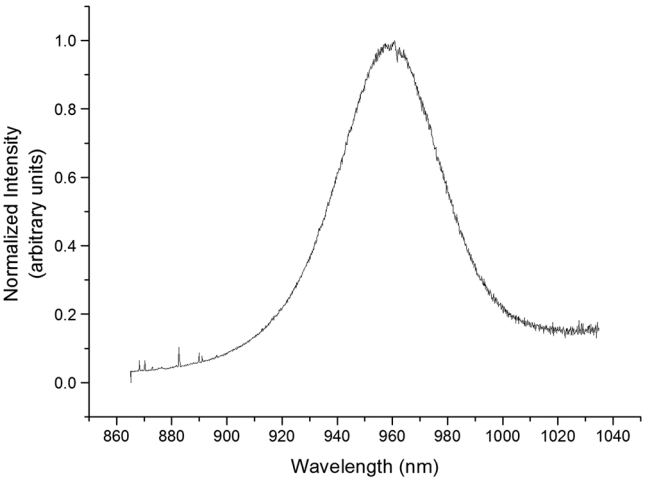

Fig. 7 SMPAF spectrum of sepia melanin. $\lambda_{exc} = 1505.9$ nm, CW.

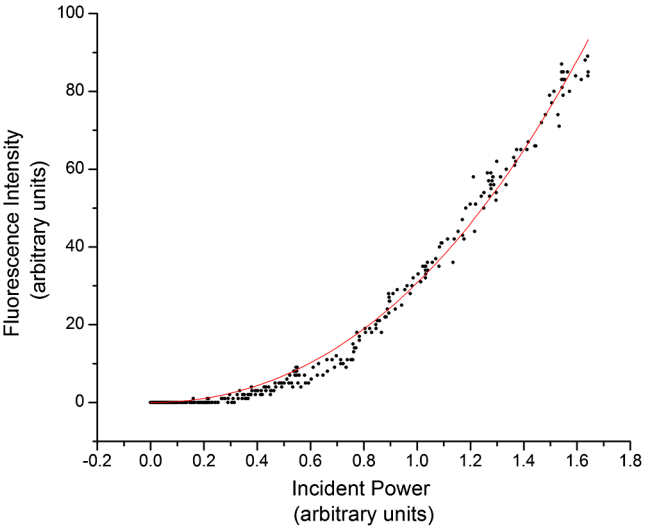

Fig. 8 Power dependence of SMPAF of mouse hair melanin. The red curve is the polynomial fit of fluorescence intensity versus incident power. $\lambda_{exc} = 920$ nm, pulsed. The filter used is the broadband filter (370 to 650 nm).

Figure 8 shows a typical power dependence of the melanin SMPAF in mouse hair. The red curve is the polynomial fit of fluorescence intensity versus incident power. The activation source is a 920-nm pulsed laser. The filter used is the broadband filter (370 to 650 nm). The polynomial fit equation is

$$F = 5.99P^3 + 24.77P^2, \tag{1}$$

where F is the fluorescence signal, and P is the input laser power. The power dependence curve does not fit into a polynomial curve with an order higher than three. The polynomial fit curve with the second and third order indicates that a two-photon process is mixed with third-order process.

4 Discussion

The broad spectrum of melanin SMPAF at visible and NIR wavelengths activated by NIR laser reveals a new and low-cost method of melanin detection. The acquired multimodal images

confirmed that this new method is reliable. The fact that SMPAF imaging has much higher SNR under CW laser excitation as a result of reduced auto-fluorescence, while a CW laser is much cheaper than the pulsed laser, indicates that this new method can be relatively low in cost. By combining CRM with SMPAF, we can locate the melanin with respect to other mouse hair and skin components.

It is unsure why the activation of melanin is not uniform. The activation of melanin doesn't appear to be polarization dependent or wavelength dependent. However, the amount of melanin activated increases with incident power and exposure time, but increased exposure causes a risk of photo-bleaching and added instability. For example, the laser power used in Fig. 5 was twice as high as that used in Fig. 4 to ensure deep laser penetration into the skin. As a result, some more melanin is activated during the imaging. Meanwhile, some activated melanin is photo-bleached, due to strong laser exposure. Therefore, the input laser power needs to be reduced after melanin is activated. In Fig. 4, six images [Fig. 4(a)–4(f)] have been taken under different modalities or filters. The interval between each image is approximately 2 min. About 10 min has elapsed from Fig. 4(a) to 4(f). The SMPAF signal locations remain the same, which is proof of the stability of the images over time.

This article is the first to report the melanin emission spectrum peak at 960 nm. Besides Teuchner's and Hoffmann's work, Huang has reported Raman spectrum of melanin from human skin peaks at 895 nm.[24] The SMPAF spectrum peak at 960 nm shows that the majority of SMPAF photons are located at the region of 940 to 980 nm. Detection of SMPAF signal near 960 nm might be a more energy efficient way of melanin detection. By lowering the incident photon energy, it is possible to detect melanin SMPAF while avoiding the damage of biological components due to high laser power. The peak of the spectrum of melanin SMPAF may also shift with the wavelength of the excitation source or with the different kinds of melanin in different biological samples. Further work is needed to confirm the feasibility of the SMPAF in the peak region of the spectrum.

Our previous work indicates that there is a possibility of obtaining a mixed spectrum of SMPEF observed by Teuchner and Hoffmann and SMPAF observed by Kerimo.[21] The SMPAF observed by Kerimo is a third-order process. The wide spectrum distribution and strong signal indicates that the SMPAF observed by Kerimo is detected in this work. The power dependence curve suggests that the fluorescence signal detected is a mixed signal of SMPAF observed previously mixed with a second-order process, which might be the SMPEF detected by Teuchner and Hoffmann. There is also a possibility that the procedures of generation of melanin SMPAF can generate a second-order process in mouse hair. Further study is needed to determine the number of photons absorbed in the activation procedure.

5 Conclusion

SMPAF images of melanin in mouse hair and skin are compared with conventional multiphoton fluorescence microscopy and CRM. SMPAF images of melanin in mouse hair and skin are background-free. Melanin is located reliably with respect to other components inside mouse hair and skin. The melanin SMPAF signal from the mouse hair is a mixture of a two-photon process and a third-order process. The melanin SMPAF emission spectrum activated by 1505.9-nm laser light is measured and shows a peak at 960 nm. Photo-bleaching during melanin detection can be reduced by detection of SMPAF around the emission peak as less laser energy is used.

Acknowledgments

This work was supported in part by CenSSIS, the Gordon Center for Subsurface Sensing and Imaging Systems.

References

1. N. Kollias et al., "Photoprotection by melanin," *J. Photochem. Photobiol. B* **9**(2), 135–160 (1991).
2. J. P. Ortonne, "Photoprotective properties of skin melanin," *Br. J. Dermatol.* **146**(S61), 7–10 (2002).
3. G. Zonios et al., "Melanin absorption spectroscopy: new method for noninvasive skin investigation and melanoma detection," *J. Biomed. Opt.* **13**(1), 014017 (2008).
4. H. Z. Hill, "The function of melanin or 6 blind people examine an elephant," *BioEssays* **14**(1), 49–56 (1992).
5. J. D. Simon and S. Ito, "The chemical structure of melanin," *Pigment Cell Res.* **17**(4), 423–424 (2004).
6. R. Robbins, *Chemical and Physical Behavior of Human Hair*, Springer, New York (2002).
7. W. Bush et al., "The surface oxidation potential of human neuromelanin reveals a spherical architecture with a pheomelanin core and a eumelanin surface," *Proc. Nati. Acad. Sci.* **103**(40), 14785–14789 (2006).
8. P. Meredith and T. Sarna, "The physical and chemical properties of eumelanin," *Pigment Cell Res.* **19**(6), 572–594 (2006).
9. J. Cheng, S. Moss, and M. Eisner, "X-ray characterization of melanins —I," *Pigment Cell Res.* **7**(4), 255–262 (1994).
10. J. Cheng, S. Moss, and M. Eisner, "X-ray characterization of melanins —II," *Pigment Cell Res.* **7**(4), 263–273 (1994).
11. S. Meng and E. Kaxiras, "Theoretical models of eumelanin protomolecules and their optical properties," *Biophy. J.* **94**(6), 2095–2105 (2008).
12. Y. Liu and J. Simon, "Isolation and biophysical studies of natural eumelanins: applications of imaging technologies and ultrafast spectroscopy," *Pigment Cell Res.* **16**(6), 606–618 (2003).
13. M. Rajadhyaksha et al., "*In vivo* confocal scanning laser microscopy of human skin: melanin provides strong contrast," *J. Investig. Dermatol.* **104**(6), 946–952 (1995).
14. I. Piletic, T. Matthews, and W. Warrena, "Estimation of molar absorptivities and pigment sizes for eumelanin and pheomelanin using femtosecond transient absorption spectroscopy," *J. Chem. Phys.* **131**(18), 181106 (2009).
15. J. Krohn et al., "Transscleral visible/near-infrared spectroscopy for quantitative assessment of melanin in a uveal melanoma phantom of *ex vivo* porcine eyes," *Exp. Eye Res.* **90**(2), 330–336 (2010).
16. X. Han et al., "Near-infrared autofluorescence imaging of cutaneous melanins and human skin *in vivo*," *J. Biomed. Opt.* **14**(2), 024017 (2009).
17. P. Meredith and J. Riesz, "Radiative relaxation quantum yields for synthetic eumelanin," *Photochem. Photobiol.* **79**(2), 211–216 (2004).
18. K. Teuchner et al., "Fluorescence studies of melanin by stepwise two-photon femtosecond laser activation," *J. Fluoresc.* **10**(3), 275–281 (2000).
19. K. Hoffmann et al., "Selective femtosecond pulse-excitation of melanin fluorescence in tissue," *J. Investig. Dermatol.* **116**(4), 629–630 (2001).
20. J. Kerimo, M. Rajadhyaksha, and C. A. DiMarzio, "Enhanced melanin fluorescence by stepwise three-photon excitation," *Photochem. Photobiol.* **87**(5), 1042–1049 (2011).
21. Z. Lai, J. Kerimo, and C. A. DiMarzio, "Melanin fluorescence spectra by step-wise three photon activation," *Proc. SPIE* **8227**, 82270J (2012).
22. Y. Mega et al., "Three-photon fluorescence imaging of melanin with a dual-wedge confocal scanning system," *Proc. SPIE* **8226**, 822637 (2012).
23. W. Warger et al., "Multimodal optical microscope for detecting viability of mouse embryos *in vitro*," *J. Biomed. Opt.* **12**(4), 044006 (2007).
24. Z. Huang et al., "Raman spectroscopy of *in vivo* cutaneous melanin," *J. Biomed. Opt.* **9**(6), 1198–1205 (2004).